Monte Carlo calculation of organ and effective doses due to photon and neutron point sources and typical X-ray examinations: results of an international intercomparison exercise.

Christelle Huet, Jonathan Eakins, Maria Zankl, Jose-Maria Gomez-Ros, Jan Jansen, Montse Moraleda, Lara Struelens, Deepak Akar, Jorge Borbinha, Hrvoje Brkic, et al.

Radiation Measurements 150 (2022) 106695

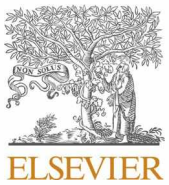

Contents lists available at ScienceDirect

Radiation Measurements

journal homepage: www.elsevier.com/locate/radmeas

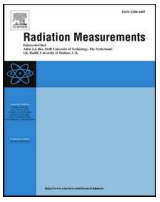

Monte Carlo calculation of organ and effective doses due to photon and neutron point sources and typical X-ray examinations: Results of an international intercomparison exercise

Christelle Huet [a,*], Jonathan Eakins [b], Maria Zankl [c], José María Gómez-Ros [d], Jan Jansen [b], Montserrat Moraleda [d], Lara Struelens [e], Deepak K. Akar [f,g], Jorge Borbinha [h], Hrvoje Brkić [i], Duc Ky Bui [j], Kevin Capello [k], Thi My Linh Dang [j], Laurent Desorgher [l], Salvatore Di Maria [h], Lior Epstein [m], Dario Faj [i], Karin Fantinova [n], Paolo Ferrari [o], Sebastian Gossio [p], John Hunt [q], Zoran Jovanovic [r], Han Sung Kim [s], Dragana Krstic [r], Ngoc Thiem Le [j], Yi-Kang Lee [t], Manohari Murugan [u], Minal Y. Nadar [f], Ngoc-Quynh Nguyen [j], Dragoslav Nikezic [r], Hemant K. Patni [f], Denison Souza Santos [q], Marilyn Tremblay [k], Sebastian Trivino [v], Katarzyna Tymińska [w]

[a] *Institute for Radiological Protection and Nuclear Safety (IRSN), Fontenay-aux-Roses, France*
[b] *United Kingdom Health Security Agency (UKHSA), Chilton, Oxfordshire, United Kingdom*
[c] *Helmholtz Zentrum München (GmbH) German Research Center for Environmental Health, Institute of Radiation Medicine, Ingolstädter Landstr. 1, 85764, Neuherberg, Germany*
[d] *CIEMAT – Centro de Investigaciones Energéticas, Medioambientales y Tecnológicas, Madrid, Spain*
[e] *SCK CEN – Belgian Nuclear Research Centre, Mol, Belgium*
[f] *Bhabha Atomic Research Centre, Mumbai, India*
[g] *Homi Bhabha National Institute, Mumbai, India*
[h] *Centro de Ciências e Tecnologias Nucleares, Instituto Superior Técnico, UL, Lisboa, Portugal*
[i] *Faculty of Medicine, Osijek, Croatia and Faculty of Dental Medicine and Health, Osijek, Croatia*
[j] *Institute for Nuclear Science and Technology, Hanoi, Viet Nam*
[k] *Health Canada, Ottawa, Canada*
[l] *Institute of Radiation Physics (IRA), Lausanne University Hospital and University of Lausanne, Lausanne, Switzerland*
[m] *Soreq Nuclear Research Center, Yavneh, Israel*
[n] *SURO (National Radiation Protection Institute), Prague, Czech Republic*
[o] *ENEA - Radiation Protection Institute, Bologna, Italy*
[p] *Autoridad Regulatoria Nuclear, Caba, Argentina*
[q] *Instituto de Radioproteção e Dosimetria/CNEN, Rio de Janeiro, Brazil*
[r] *University of Kragujevac, Faculty of Science, Kragujevac, Serbia*
[s] *Korea Institute of Radiological and Medical Sciences (KIRAMS), Seoul, South Korea*
[t] *Université Paris-Saclay, CEA, Service D'Études des Réacteurs et de Mathématiques Appliquées, 91191, Gif-sur-Yvette, France*
[u] *Indira Gandhi Centre for Atomic Research, Kalpakkam, India*
[v] *CNEA, Comisión Nacional de Energía Atómica, Argentina*
[w] *National Centre for Nuclear Research, Otwock, Poland*

ARTICLE INFO

Keywords:
Monte Carlo
ICRP reference phantom
Organ absorbed dose

ABSTRACT

This paper summarizes the results of an intercomparison on the use of the ICRP Reference Computational Phantoms with radiation transport codes, which was organized by EURADOS working group 6. Three exercises are described: exposure to an anterior-posterior (AP) photon point source, exposure to an AP neutron point source, and exposure to two typical medical X-ray examinations. The three exercises received 17, 8 and 8 solutions, respectively. Participants originated from fifteen different countries, and used a wide range of Monte Carlo codes. Due to difficulties in defining the precise source location unambiguously in the exercise description, agreement to within ~10% of the reference solution was considered satisfactory for a given participant's results. Although some participants provided initial solutions in good agreement with the reference solutions, differences

* Corresponding author.christelle.huet@irsn.fr

https://doi.org/10.1016/j.radmeas.2021.106695
Received 30 June 2021; Received in revised form 3 December 2021; Accepted 6 December 2021
Available online 9 December 2021

of several tens of percent, or even several orders of magnitude, were exhibited for many of the others. Following feedback and suggestions from the organizers, revised solutions were submitted by some of the participants for the photon exercises; in general, agreement was improved. The overall observations from these three intercomparison exercises are summarized and discussed.

1. Introduction

In the framework of EURADOS[1] working group 6 (WG6) on computational dosimetry (Rabus et al., 2021), an intercomparison was organized on the usage of the ICRP[2] Reference Male (RMCP) and Female (RFCP) Computational Phantoms together with radiation transport codes. Six different exercises of practical interest in occupational, environmental and medical dosimetry were proposed (Zankl et al., 2021a). Participants were asked to evaluate specific dose quantities and report their results to the organizers for comparison against verified reference values. The principal aims of this intercomparison exercise were to investigate how well the phantoms have been implemented by the participants in their models, and to allow participants to check their calculations against quality-assured reference solutions.

This paper focuses on three of those exercises: exposure to an AP photon point source, exposure to an AP neutron point source, and exposure to two typical medical X-ray examinations. First, the configurations that were to be modelled are described. Next, the solutions initially provided by the participants are presented and compared against the reference solutions. Where appropriate, these are then followed by the analysis of the solutions received after feedback to the participants regarding their initial solutions. Finally, discussion is given on the general trends and common errors made by the participants.

2. Material and methods

2.1. Description of the problems

In each case, it was recommended that participants use the reference computational phantoms as described in ICRP Publication 110 (ICRP, 2009), with the organ and tissue masses that are given therein. For red bone marrow (RBM) and endosteum (bone surface) dosimetry, the method proposed in ICRP Publication 116 (ICRP, 2010) was recommended: that is, application of dose response functions or dose enhancement factors. For the calculation of effective doses, the tissue weighting and radiation weighting factors from ICRP Publication 103 (ICRP, 2007) were presumed. Along with their results, participants were requested to state explicitly the method of bone dosimetry that they had used, and asked to explain in detail any method that deviated from that of ICRP Publication 116.

2.1.1. Photon and neutron point source exercises

The photon and neutron point sources problem were specified according to the following description:

- An isotropic Co-60 or neutron point source was placed in front of the reference voxel phantom.
  - o For the Co-60 source, only the gamma emission was considered. The source activity was 10 GBq.
  - o For the neutron, the source was assumed to emit 10 keV neutrons with an activity of 1 GBq.
- The point source was at 125 cm from the bottom of the feet of the phantom and at 100 cm from the chest.
- The configuration was surrounded by vacuum. It is illustrated in Fig. 1.

Regarding the Co-60 source, participants were tasked with reporting the organ absorbed doses from a 10 min exposure time to the RBM, colon, lungs, stomach, breast, testes/ovaries, liver, oesophagus, brain and skin of both the RMCP and RFCP, as well as the overall effective dose.

Regarding the 10 keV neutron source, participants were tasked with reporting the organ absorbed doses from a 1 min exposure time to the RBM, stomach, small intestine, testes/ovaries, liver, brain and skin of both the RMCP and RFCP, as well as the overall effective dose.

2.1.2. Typical X-ray examinations

Two typical X-ray examinations were designed: a chest postero-anterior (PA) and an abdomen antero-posterior (AP). A divergent rectangular energy-spectral X-ray source (point source) was placed behind and in front of the reference voxel phantom for the chest PA and abdomen AP configurations, respectively, and directed towards it (Fig. 2). An imaginary rectangular image receptor was placed in front of and behind the phantom for the chest PA and abdomen AP configurations, respectively. Details on all relevant distances, the field size at the detector, the field position (Table 1), and the X-ray spectra (Chest PA: 125 kVp, 2.5 mm Al filtration; Abdomen AP: 90 kVp, 2.5 mm Al filtration) were provided to the participants.

For both male and female phantoms, participants were asked to determine the coordinates of the X-ray source and to calculate the organ absorbed doses normalized to entrance air kerma free-in-air and to

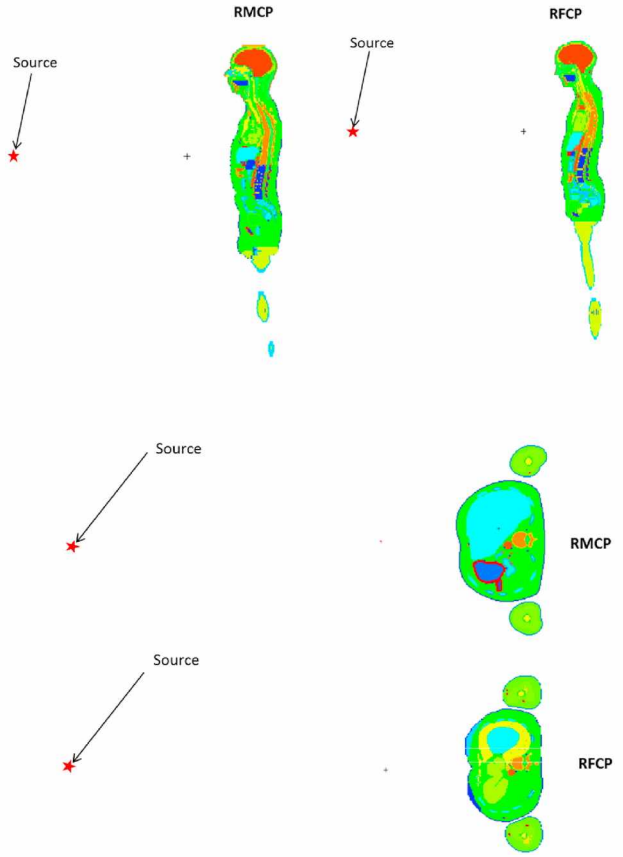

Fig. 1. Illustration of point source position relative to RMCP (male) and RFCP (female) phantoms.

[1] European Radiation Dosimetry group.
[2] International Commission on Radiological Protection.

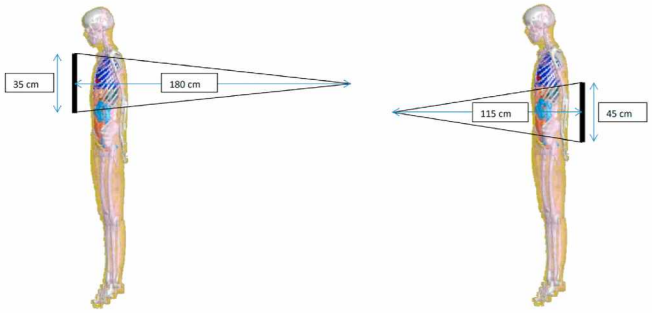

Fig. 2. PA chest (left) and AP abdomen (right) examinations.

Table 1
Parameters used for Chest PA and Abdomen AP X-ray examinations.

X-ray examination	Point source to image receptor distance (cm)	Skin to detector distance (cm)	Field size at the receptor (width x height) (cm x cm)	Lateral field centre	Vertical field centre
Chest PA	180	10	35 × 35	Between left-most and right-most extensions of the lungs	Between top and bottom extensions of the lungs
Abdomen AP	115	10	35 × 45	Between left-most and right-most extensions of the pelvic bone	Between top of the liver and bottom of the pelvic bone

kerma-area-product for: the RBM, lungs, stomach, breast, heart, oesophagus and thyroid for the chest PA examination; and for the RBM, liver, kidneys, pancreas, small intestine, colon and bladder wall for the abdomen AP examination.

2.2. Analysis of the solutions

At least two members of EURADOS WG6 coordinated each exercise. The task was first completed by one of these persons to generate a reference solution. Then it was independently completed by the other involved member or members to confirm the accuracy of that reference solution. For each organ and effective dose, agreement of the two solutions to within a few percent was considered evidence of acceptable conformity, taking account of the respective statistical uncertainties on the results. The Monte Carlo codes used for the setting of the reference solutions are listed in Table 2.

Template spreadsheets were provided to participants, in which they could enter their solutions in a pre-defined format to facilitate the evaluation process. Additional information was also asked from them, such as the transport code and the method of bone dosimetry that were used and whether the kerma approximation was adopted.

The solutions achieved by the participants were compared with the reference one. In those cases where large discrepancies were found, the results were examined closely and, for the photon exercises (Co-60 and X-ray), bespoke feedback was provided to the participants and a revision was requested to find out the reasons for the discrepancy. For those cases still requiring further revision, additional feedback was given to the participants, and in a few cases the complete input for the Monte Carlo code or their post-processing files were checked by the organizers to find out the mistakes. Conversely, feedback was not provided for the neutron exercise, nor revised submissions requested. This is partly because every participant who contributed a solution to that exercise had also contributed a solution to at least one other of the exercises described in (Zankl et al., 2021a), and it was apparent that in many cases, the problems encountered by the individuals were likely being repeated, leading to similar errors being made; it is therefore probable that the feedback and suggestions that would have been appropriate had already been provided elsewhere.

3. Results

Seventeen, eight and eight solutions were received for the photon point source, the neutron point source and the X-ray examination exercises, respectively. These are identified by the randomly allocated letters a to r in the following, with all results therefore presented anonymously; where a given participant submitted a solution for more than one of the three exercises, however, the same letter has been allocated in each case. The participants originated from fifteen different countries: Argentina, Brazil, Canada, Croatia, Czech Republic, France, India, Israel, Italy, Poland, Portugal, Serbia, South Korea, Switzerland and Vietnam. The computer codes, particle transport options and cross-section data reported by the participants are summarized in Table 3. The MCNP family of codes (Werner et al., 2017) was the most widely adopted, with eleven participants using one of those versions. Regarding the seven remaining solutions, a large variety of Monte Carlo codes was used (FLUKA (Battistoni et al., 2006), Geant4 (Agostinelli et al., 2003), PenEasy (Sempau et al., 2011), TRIPOLI-4 (Brun et al., 2015) and VMC (Hunt et al., 2004)). The RBM dosimetry method used by the participants is given in Table 4. The majority of participants (11) reported that they used the method described in ICRP 116. However, among them, three participants did not specify which ICRP116 method. The 'home-made' method employed by one of the participants for RBM dosimetry was not described further.

3.1. Photon point source exercise

3.1.1. Reference solution

The organ absorbed doses and effective dose data that were

Table 2
Monte-Carlo codes used by the organizers for the initial determination (*top of each row*) and verification (*middle* and *bottom of each row*) of the reference solutions. For the neutron point source exercise and the X-ray examinations exercise, two verifications were performed.

Exercise	MC code	Kerma approximation	Cross-section library		
			Photon	Electron	Neutron
Co-60 point source	MCNPX 2.6c	No	mcplib04	el03	–
	EGSnrc	No	XCOM database	NIST Bremsstrahlung cross sections	–
Neutron point source	MCNPX 2.7	Yes	mcplib84	el03	ENDF70
	MCNPX 2.7	Yes	mcplib84	el03	ENDF80
	MCNP6.1	Yes	mcplib84	el03	ENDF70
X-ray examinations	EGSnrc	No	XCOM database	NIST Bremsstrahlung cross sections	–
	MCNPX	No	mcplib84	el03	–
	MCNP	Yes	mcplib84	el03	–

Table 3
Summary of Monte-Carlo codes and cross-section libraries used by the participants.

Code	Number of solutions	Kerma Approximation	Cross-Section Library		
			Photon	Electron	Neutron
MCNPX (2.6.0 or 2.7.0)	5	Yes[a] (2) No[a] (5)	mcplib04 mcplib84 ENDF71	el03	ENDF70a
MCNP6 (6.1 or 6.2)	4	Yes (1) No (3)	mcplib84	el03	ENDF/B-VI.8 ENDF71x
MCNP4c3	1	Yes	mcplib04	el032	-
MCNP	*1*	*No*	unspecified	*unspecified*	-
Visual Monte Carlo version 2018	1	Yes	*NIST XCOM*		-
FLUKA	2	No	EPDL 97	FLUKA algorithm + Seltzer & Berger model	FLUKA multigroup
TRIPOLI-4	1	No	EPDL 97	EEDL + Brem	JEFF-3.3
PenEasy 2015	1	No	EPDL 97	Seltzer & Berger model	
Geant4 (10.04.p01 and 10.4)	2	No	Livermore EPDL 97	Livermore EEDL	ENDF/B-VII ENDFVII.0

[a] 2 participants submitted two solutions: one with and one without the kerma approximation.

Table 4
Summary of the RBM dosimetry method used by the participants.

RBM Method	Number of solutions	Participants
ICRP 116 (method unspecified)	3	m, p, r
Dose response functions (ICRP 116)[a]	6	c, h, i, j, l, o
"Three-factor method" (ICRP 116)[a]	2	b, n
Mass- weighted spongiosa doses	4	a, d, e, k
ICRP 103	1	q
Homemade method	1	f
No bone dosimetry	1	g

[a] Detailed in (Zankl et al., 2021b).

generated by the organizer with MCNPX 2.6 code (Table 2) are presented in Table 5. A possible source of inaccuracy results from the choice of the location of the point source, as the instruction that was given to participants was to place it '100 cm from the surface of the chest', which could be interpreted differently. A sensitivity analysis on the source location was performed by the organizer. It consisted of repeating the calculations for both male and female phantoms with a source location translated 2 cm and 5 cm nearer or further to the body in the horizontal plane. The resulting organ absorbed doses were respectively increased or decreased by the source displacement, by up to 10% depending on the organ and the distance considered. Considering that, the solution was accepted as correct if the agreement was within 10%.

3.1.2. *Initial solutions*

The following radiation transport codes were used by the participants: FLUKA (2 participants), Geant4 (2 participants), MCNP (5 participants), MCNPX (6 participants), TRIPOLI, and VMC. The organ absorbed dose results that were submitted by the seventeen participants are shown in Fig. 3 for the male phantom and in Fig. 4 for the female phantom, along also with the reference results. In both cases, the left figure shows all of the data that were submitted, and the right figure shows that same data on a restricted x-axis that serves to remove the most extreme outliers. The standard deviation statistical uncertainties on the results are not shown on the figures for clarity, but were no more than a few percent. Participants a and e provided two solutions: one derived with the kerma approximation and a second without. Regarding solution f, only results for the female phantom were provided by the participant.

Table 5
Reference organ absorbed doses and effective dose for the Co-60 point source. Standard statistical uncertainties are also indicated.

	Organ absorbed doses (Gy) and effective dose (Sv)			
	Male		Female	
	Dose (Gy)	*std. unc. (%)*	*Dose (Gy)*	*std. unc. (%)*
RBM	3.26×10^{-4}	0.34	3.68×10^{-4}	0.39
Colon	4.09×10^{-4}	0.59	4.53×10^{-4}	0.57
Lungs	3.84×10^{-4}	0.22	4.05×10^{-4}	0.27
Stomach	4.30×10^{-4}	0.42	4.69×10^{-4}	0.42
Breast	5.36×10^{-4}	2.15	5.60×10^{-4}	0.50
Testes/Ovaries	3.91×10^{-4}	1.37	3.50×10^{-4}	1.27
Liver	3.86×10^{-4}	0.15	4.39×10^{-4}	0.16
Oesophagus	3.69×10^{-4}	0.87	4.18×10^{-4}	0.89
Brain	2.81×10^{-4}	0.19	3.40×10^{-4}	0.19
Skin	2.60×10^{-4}	0.22	2.70×10^{-4}	0.23
Effective dose	$4.18 \times 10^{-4} \pm 0.45\%$			

For the male phantom, eight (a without kerma approximation, e without kerma approximation, h, i, k, l, o and r) out of the seventeen participants provided results that agreed well (within 7.5%) with the reference solution for all the organs investigated. For five solutions (a with kerma approximation, b, c, e with kerma approximation and p), an agreement better than 6.5% with the reference solution was also observed for all the organs except for the skin. For this latter, absorbed dose is overestimated by around 20% by the participants compared to the reference solution, except for solution c for which the overestimation is around 95%. An underestimation of around 50% is observed for solutions d and n for all the investigated organs, except for the gonads for Participant n (overestimation of nearly 4%). Regarding solution j, the relative difference from the reference solution is below 11% except for the RBM dose, which is fifteen-fold the reference value. Large discrepancies are observed for solution m for the colon (85%), the stomach (90%), the breast (150%) and the skin (21%), whereas for the other organs the differences are around 4%. Finally, for solution q, differences range from −90% (liver) to 950% (RBM).

For the female phantom, five (a without kerma approximation, h, k, o and r) out of the seventeen participants provided results that agreed well (within 5.3%) with the reference solution for all the organs investigated. For four solutions (a with kerma approximation, b, c and p), an agreement better than 3.3% with the reference solution was also observed for all the organs except for the skin. For this latter organ, compared to the reference solution, absorbed dose is overestimated by around 30% by participants a and b, 17% for Participant p, and 125% for Participant c. Regarding solution l, a good agreement is observed for all the organs investigated (relative difference <3%) except for the ovaries (10%). Organ absorbed doses are underestimated by around 10% for both solutions e (with and without kerma approximation), except for the skin for the solution with the kerma approximation, for which an overestimation of around 20% is observed. Regarding solution f, a good agreement is observed for all the organs investigated (relative difference <5%) except for the RBM (30%). Absorbed doses provided by Participant i for RBM and ovaries are overestimated (14%) and underestimated (13%) respectively. An underestimation of around 50% is observed for solutions d and n for all the investigated organs. Regarding solution j,

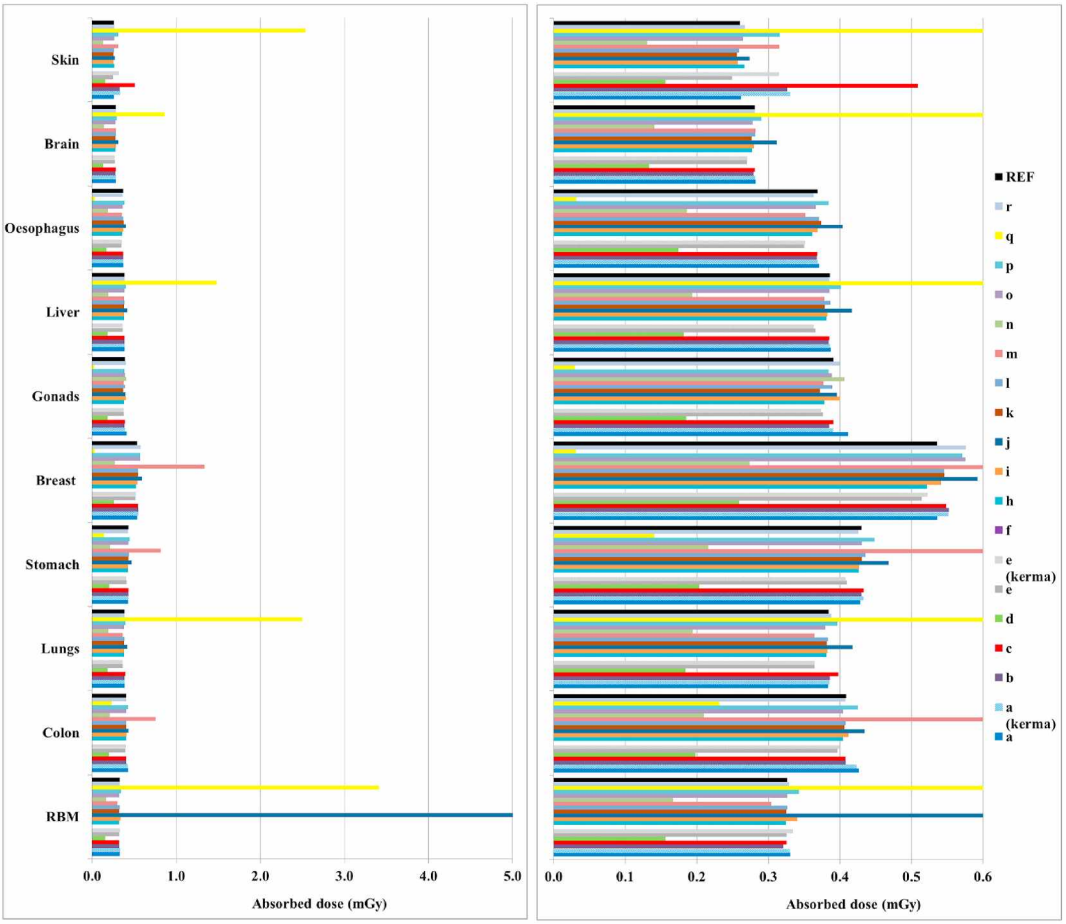

Fig. 3. Photon point source exercise - Initial organ absorbed dose for the male phantom compared with reference data. (Left) all data; (Right) excluding extreme outliers. Participants a and e provided two solutions: one derived with the kerma approximation, noted a (kerma) and e (kerma), and a second without, noted a and e.

the relative difference with the reference solution is below 1.2% except for the RBM dose, which is fourteen-fold the reference value. Large discrepancies are observed for solution m for nearly all the organs investigated, and for solution q for all the organs.

The effective dose results, $E(P)$, that were submitted by the participants are shown in Fig. 5 as ratios, $E(P)/E(O)$, to the reference effective dose, $E(O)$. The standard deviation statistical uncertainties on the results are again not shown on the figure for clarity, but were no more than a few percent. Participant d provided solutions for the male and female phantoms individually instead of the correct sex-averaged quantity. Regarding Participant f, as organ absorbed doses were computed for the female phantom only, the quantity assessed is the one taking into account the female phantom only.

Twelve participants (a, b, c, e, f, h, i, k, l, o, p and r) submitted solutions for effective dose agreeing to within a few percent with the reference solution. Of the five solutions (d, j, m, n and q) where large differences are observed for effective dose, large differences were also observed for organ absorbed doses. Regarding solutions d and n, effective dose is once again half the reference value. However, it is interesting to observe that the effective doses computed by participants who had only one organ absorbed dose in disagreement with the reference value (solution c for instance) are in good agreement with the reference value. One explanation could be the weighting process, which reduced the impact of individual organ results that were too high or too low.

The analysis of the results revealed that for several solutions, organ absorbed doses were systematically a few % higher (for instance solution p for male phantom) or lower (for instance solution m for male and female phantoms) than the reference ones. Some participants provided their point source position and it is likely that these differences were attributable to the location of the source. Finally, regarding the overestimations of skin absorbed dose of around 20% and 30% for the male and female phantoms, respectively observed for several solutions, it was directly linked to the use of the kerma approximation.

3.1.3. *Revision of solutions*

Taking into account the previous comments regarding, on one hand, the choice of the source location, and on the other hand the use of the kerma approximation, ten and eight participants provided an initial set of results that agreed with the reference solution (within 10%) for the male and female phantoms, respectively. Feedback was provided to all participants. For those whose solution had discrepancy with the reference solution (6 for the male phantom and 9 for the female phantom), information was provided in order to help them to find their errors. For instance:

- "Your results for the organ absorbed doses are over- or underestimated depending on the organs (with differences up to 1000% with the reference solution)."
- "Your results for the organ absorbed doses and effective dose are half the reference values."
- "Your results for the organ absorbed doses are in good agreement with the reference solution except for RBM doses for both male and female, which are overestimated (relative difference of 1000% with the reference solution). Effective dose also differs from the reference solution."

Finally, they were invited to submit a revised set of results. For a couple of them, their input file or post-processing file was studied by the

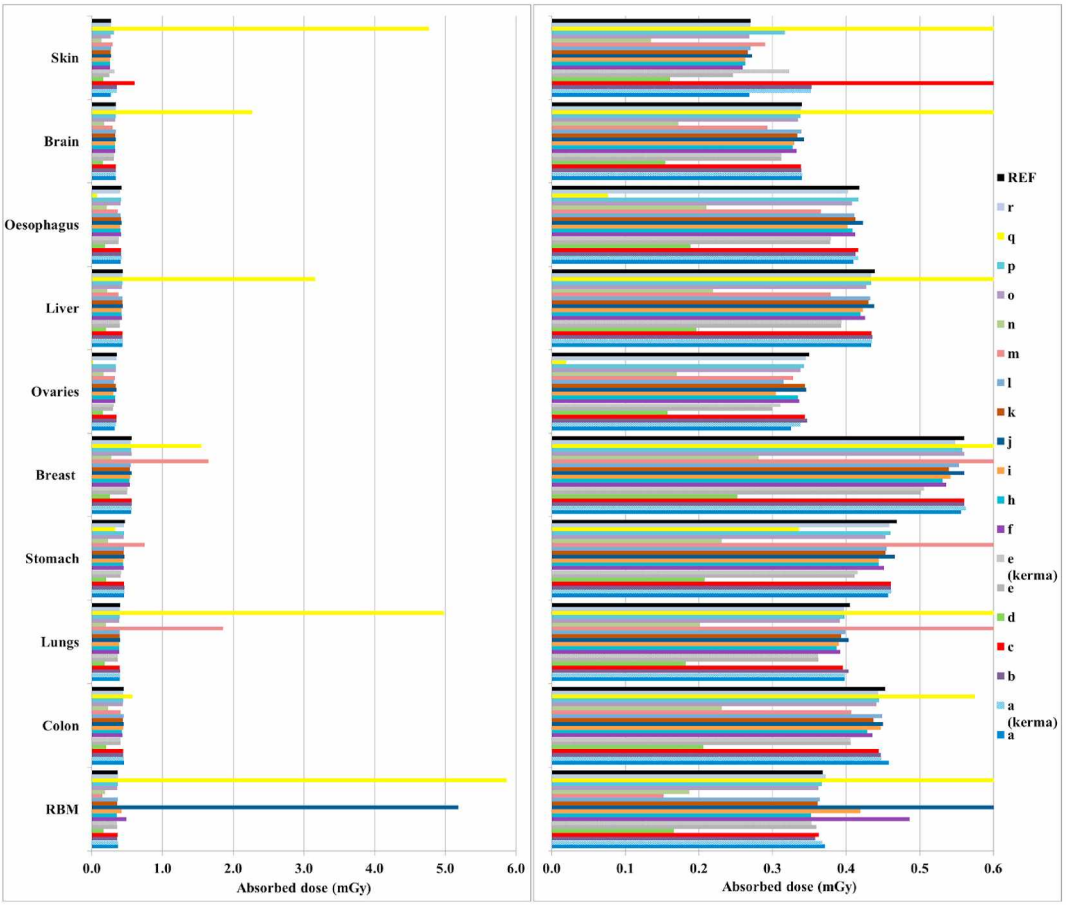

Fig. 4. Photon point source exercise - Initial organ absorbed dose for the female phantom compared with reference data. (Left) all data; (Right) excluding extreme outliers. Participants a and e provided two solutions: one derived with the kerma approximation, noted a (kerma) and e (kerma), and a second without, noted a and e.

organizer in order to help them to fix their error. Thus, for those participants, several steps and email exchanges were needed.

Six and seven revised solutions were received for the male and female phantoms respectively. In addition Participant f, who did not provide results for the male phantom during the initial submission, sent a solution for that during this revision stage.

The revised results are shown in Fig. 6 for the male phantom and in Fig. 7 for the female phantom, along also with the reference results. The revised effective dose results are shown in Fig. 8. Regarding the male phantom, a good agreement is observed for almost all the participants (15). The doses to the breast and stomach are overestimated by Participant m, while the gonads absorbed dose is overestimated by Participant n. Regarding the female phantom, an agreement to better than 15% is observed for all participants and all organs, except for RBM and stomach for Participant m. Finally, effective doses are within 15% of the reference solution except for Participants m and q.

Some of the participants identified their errors without help, whereas for others it was necessary to guide them. Finally, some of the participants gave no information about the changes they made to obtain the revised solutions. The errors can be summarized as follows:

- for five participants the method used to calculate RBM absorbed dose was wrong,
- two participants did not take into account the emission probability of the Co-60 source,
- one participant included the beta decay of Co-60 in addition to the photon decay,
- one participant reported a mistake in their calculation of absorbed dose for organs having multiple organ voxel numbers,
- one participant used the wrong tally, specifically a pulse-height tally (MCNP f8) rather than an energy deposition tally (MCNP *f8). In addition, there were copy/paste errors in the post-processing file.

Thus, most of the participants failed in implementing ICRP methodology for the assessment of RBM dose.

3.2. Neutron point source exercise

3.2.1. Reference solution

To determine effective dose, it is necessary to weight and sum the organ doses deposited by all radiation field components with tissue (w_T) and radiation (w_R) weighting factors, and then average over both sexes. The recommended scheme is detailed in ICRP 103 (ICRP, 2007), with the tissue weighting factors provided in Table B2 therein. Because the configuration is surrounded by vacuum in the current exercise, only mono-energetic neutrons are externally incident upon the phantom. However, the fields through the internal organs will be mixed, with contributions from secondary photons as well as the neutrons (plus also very short-ranged recoil protons etc., if they were being transported), and also electrons if the kerma approximation is not being applied; use of the kerma approximation was optional but valid in this case, due to the short ranges of any secondary electrons produced within the body. The radiation weighting factors are species-dependent; a flat value of $w_R = 1$ is considered valid for all incident photons (and electrons), but w_R is energy-dependent for neutrons. However, the radiation weighting factor for a given dose-depositing particle is assigned either the value corresponding to the energy it had when it was incident upon the body, or else the value appropriate for the energy of the particle that originally

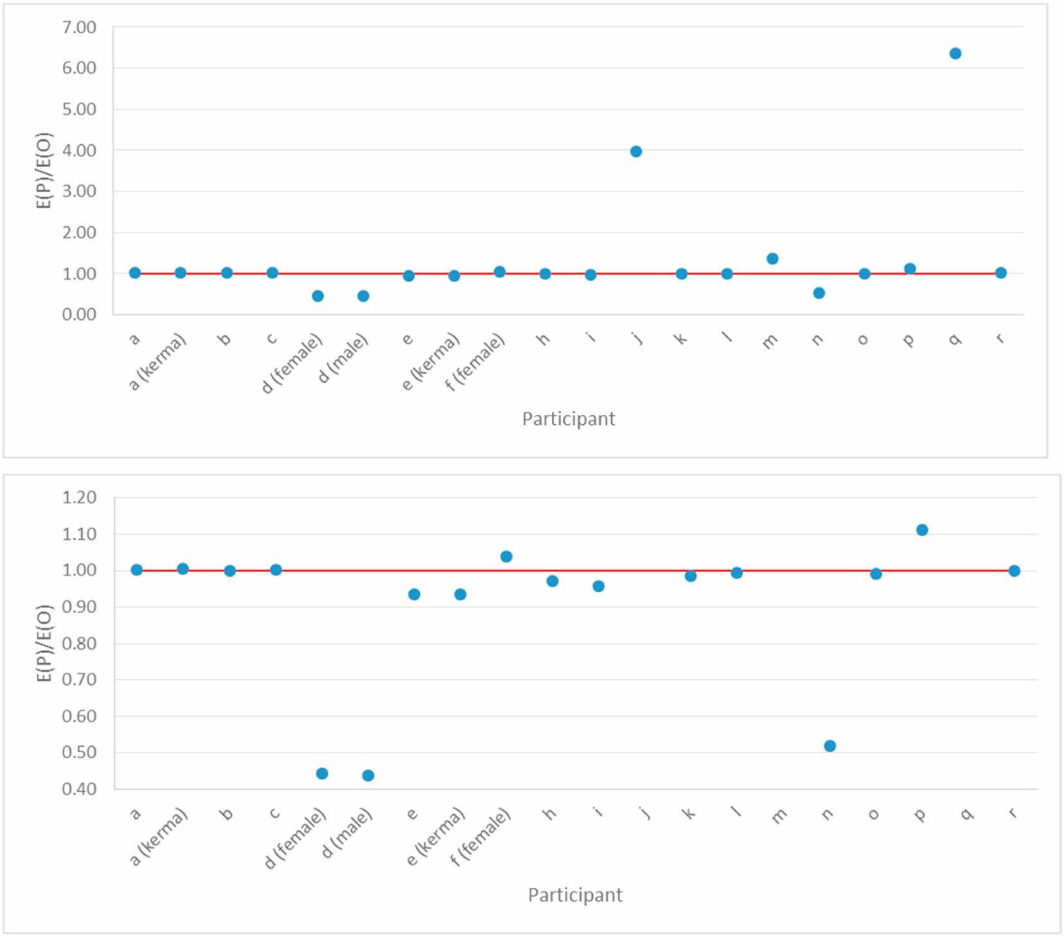

Fig. 5. Photon point source exercise - Ratio of initial effective dose data (E(P)) submitted by the participants to the reference effective dose (E(O)). (Top) all data; (Bottom) excluding extreme outliers. Participants a and e provided two solutions: one derived with the kerma approximation, noted a (kerma) and e (kerma), and a second without, noted a and e.

produced it when that parent particle was incident upon the body. In the current exercise, therefore, all doses need to be weighted by the w_R for 10 keV neutrons, even though that might seem counter-intuitive for the photon (and electron) components, because only those source neutrons were incident upon the phantoms.

To determine the correct value for w_R, Equation (1) should be applied, extracted from Equation B.3.16 in ICRP 103:

$$w_R = 2.5 + 18.2e^{-[ln(E_n)]^2/6} \quad (1)$$

which is valid when $E_n < 1$, where E_n is the neutron energy in units of MeV. In the current case of 10 keV neutrons, then $E_n = 0.01$ MeV, giving $w_R = 3.031$.

The organizer employed the Monte Carlo code MCNPX version 2.7 to perform the calculations, assuming coupled neutron-photon transport under the assumption of the kerma approximation. The ENDF70, MCPLIB84 and EL03 cross-section libraries were used for neutron, photon and electron interactions, respectively (Table 2). For the thermal cross-section treatments of the hydrogenous tissues comprising the organs, and specifically to cope with the impacts of molecular bonding on the scattering of thermalized neutrons, the organizer assumed an O–H bond equivalent to that in light water.

The reference organ and effective dose data that were generated are presented in Table 6. The neutron and photon components of these various doses are not shown separately here, but the organizer can report that they were greatly dominated by the latter: typically, the photon dose to a given organ was around an order of magnitude larger than the concurrent neutron dose. Also shown are the relative standard uncertainties on the results, relating just to the statistical fluctuations within the Monte Carlo code. The relative standard uncertainty of 0.1% for the effective dose was calculated in quadrature from the statistical uncertainties on the twenty-nine weighted organ doses used in its definition (ICRP, 2007).

The systematic uncertainties on the results are harder to quantify than the statistical uncertainties, and result from factors such as uncertainties in the cross-sections, physics models, or thermal treatment options. One additional source of inaccuracy results from the choice of location to place the source: the human body is non-uniform, making the definition of a precise reference position somewhat difficult. Accordingly, the instruction to place the source '125 cm from the feet and 100 cm from the surface of the chest' gives rise to inevitable ambiguity, with the organizer and participants all likely to interpret its exact position slightly differently. This is significant, because the inverse-square divergence of the field will cause variations in the organ doses depending on their distances from the source.

To evaluate the potential impacts of such small displacements, the calculation for the female phantom was repeated but with the neutron source translated 5 cm nearer to the body in the horizontal plane and 5 cm lower in a vertical plane. Although somewhat arbitrary, these 5 cm repositionings defined an 'envelope' that was considered a reasonable estimate of the maximum plausible ambiguity in source location relative to the body. Moreover, focus on the female phantom was adopted because, being smaller, its organs are closer to the source on average; doses are therefore more affected by perturbations in the source location than would be the case for the male, leading to a more conservative

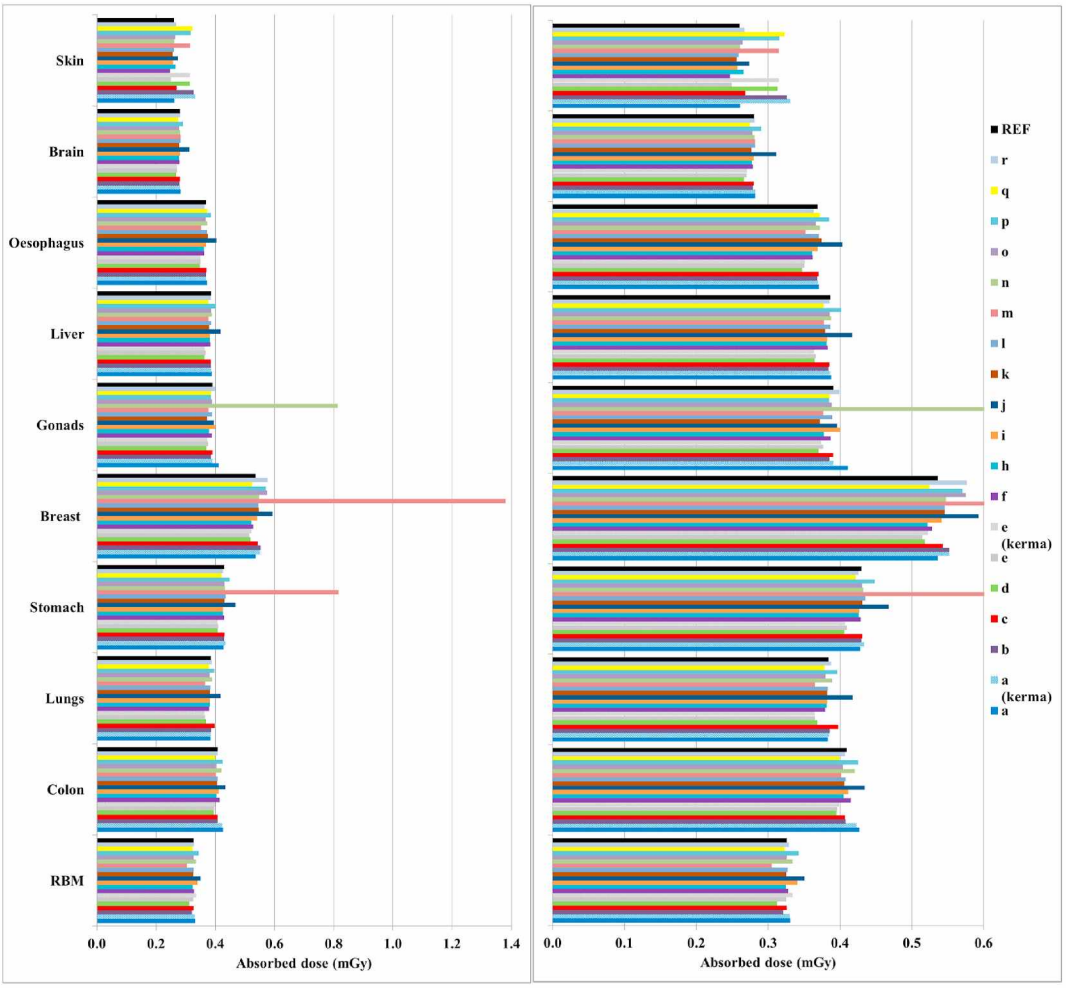

Fig. 6. Photon point source exercise - Revised organ absorbed dose for the male phantom compared with reference data. (Left) all data; (Right) excluding extreme outliers. Participants a and e provided two solutions: one derived with the kerma approximation, noted a (kerma) and e (kerma), and a second without, noted a and e.

estimate of this uncertainty component. In all cases, the resulting organ doses were increased by the source displacement, as expected from a consideration of the geometry, with the largest increase being for the ovaries (~13%) and the smallest for the brain (~4%). On average, the seven organ doses of interest changed by ~10%. Considering also the statistical uncertainties, this led to the suggestion that for the subsequent purposes of analyses of participants' results, congruence with the reference solutions to within ±10% could be taken to indicate broadly acceptable agreement, noting that there is a degree of subjectivity in this metric.

3.2.2. *Participant results*

In total, eight participants submitted solutions for this neutron problem; these used FLUKA (1 participant), Geant4 (2 participants), MCNP (4 participants) and TRIPOLI (1 participant). The computer codes, particle transport options, cross-section data and RBM dosimetry methods that were reported by the eight participants are summarized in Tables 3 and 4, with the analogous details used in the generation of the reference solutions by the organizer given in Table 2. Generally, the participants used the latest cross-section libraries that were available to them. Not shown in Table 3, nor requested from the participants, are details on any molecular bonding treatments that might have been applied to account for thermal neutron scattering. One participant provided an updated set of results, having noticed a mistake in the RBM values of their initial dataset; only this resubmitted solution is included and discussed here, on the grounds that it was quickly self-identified without any prompting or feedback from the organizer.

The organ dose results that were submitted by the eight participants are shown in Fig. 9 for the male phantom and in Fig. 10 for the female phantom, along also with the reference results. In both cases, the left plot shows all of the data that were submitted, whilst the right plot shows the same data on a partially restricted x-axis that removes the most extreme outliers; the exact ranges used in the latter two cases were chosen somewhat arbitrarily. The statistical uncertainties that were reported by the participants along with their results are not provided on the figures for clarity, but these relative 1 standard deviations were generally a few percent or less.

Participant a submitted two solution sets, one of which used coupled neutron-photon transport whilst the other employed neutron-only transport; their results from the two methods were statistically irresolvable, so for convenience only the former are discussed here. However, despite their self-consistency, this participant underestimated the reference values by about an order of magnitude. This indicates a significant error in their methodology, and it might be speculated that perhaps neither dataset properly accounted for the photon component: as mentioned previously, the organizer found the neutron dose to a given organ to be about a tenth of that from photons. Conversely, Participant i overestimated the reference values by a factor of a few, apart from their RBM doses, which were about half the reference values. Participant d underestimated most of the reference values by around two orders of magnitude, although their skin results were less than 1 order of magnitude too low, whilst the result for the ovaries was four orders of

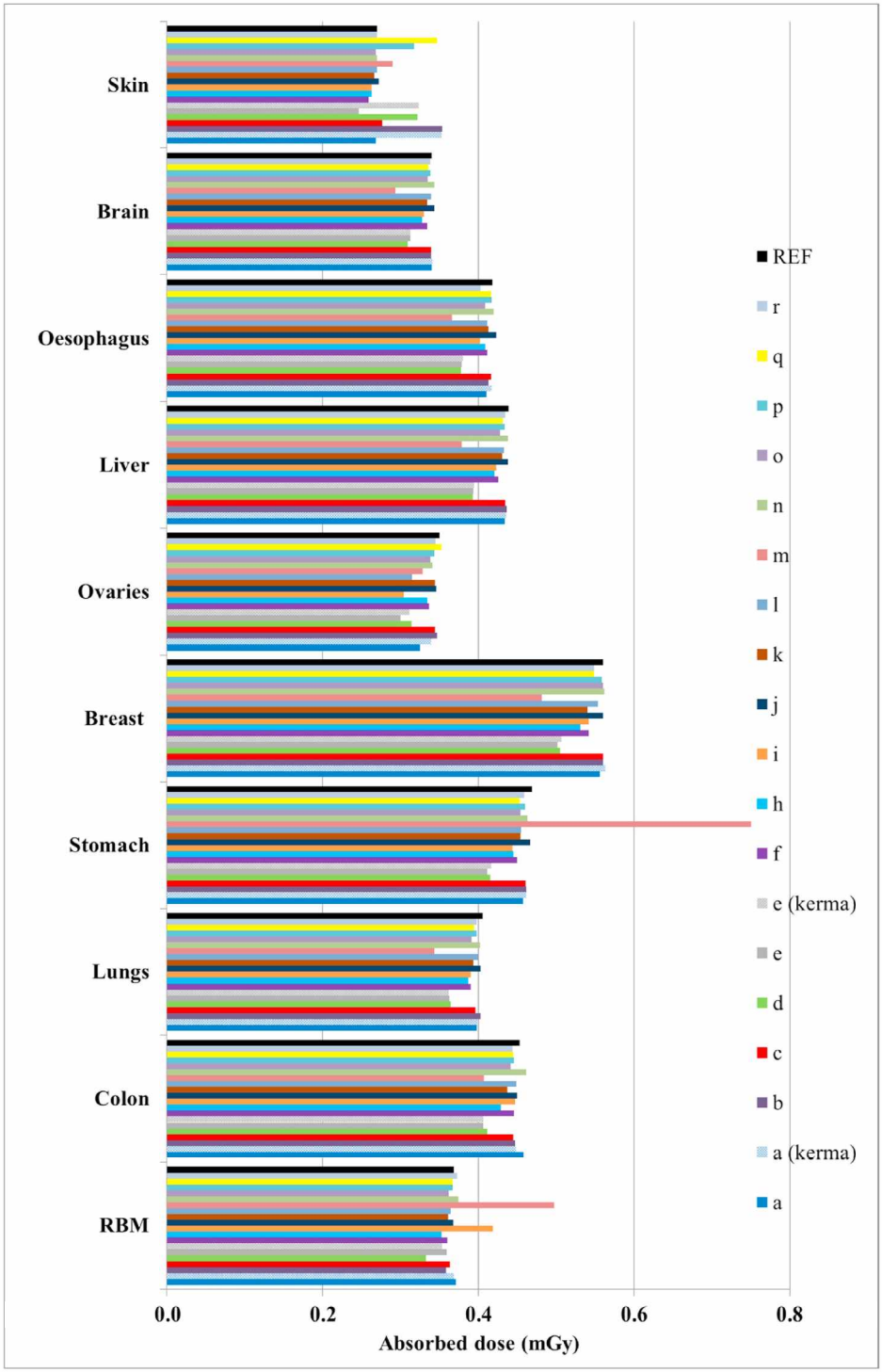

Fig. 7. Photon point source exercise - Revised organ absorbed dose for the female phantom compared with reference data. Participants a and e provided two solutions: one derived with the kerma approximation, noted a (kerma) and e (kerma), and a second without, noted a and e.

magnitude too low. The causes of these divergences are unknown, with errors in the source definition, particle transport or organ dose normalizations all plausible speculations, but are particularly puzzling for the latter outlier given its apparent inconsistency with the rest of the participant's dataset. Even when the most obvious outliers are excluded, there is still a very wide range of results from the participants. In general, a broadly similar spread is exhibited in the male and female datasets, indicating as expected that neither phantom is any more 'troublesome' to use than the other. Of all the organs, the RBM caused the most discrepancy, both in terms of general magnitude and frequency; this observation is perhaps unsurprising, given the more complex nature of RBM dosimetry compared to the other organs (ICRP, 2010). Only two of the participants (c and k) agreed with the reference values within the permitted uncertainty budget for all seven organs of both phantoms; Participant f would have done also, if RBM doses were excluded. Participant h also came close, with all organ doses lower than the reference values by up to ~20%. Participant j performed similarly to Participant h, though their RBM doses were about a third of the

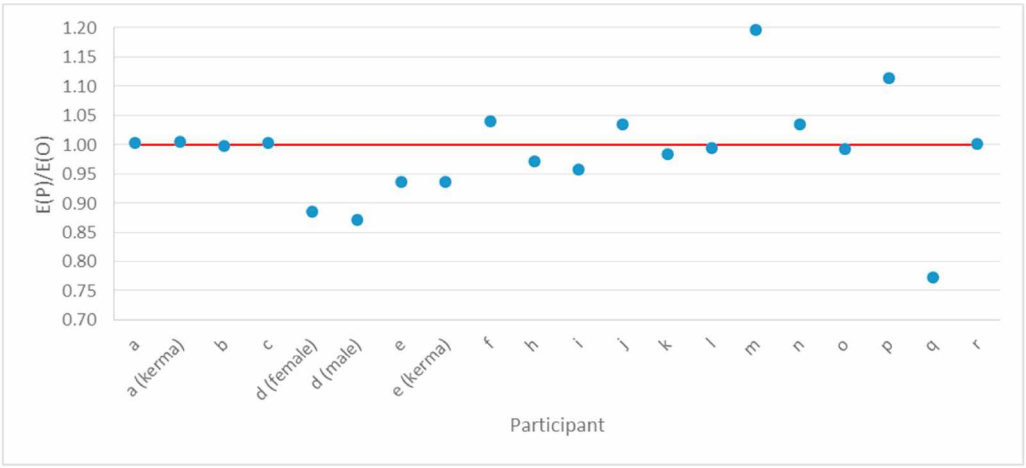

Fig. 8. Photon point source exercise - Ratio of revised effective dose data (E(P)) submitted by the participants to the reference effective dose (E(O)). Participants a and e provided two solutions: one derived with the kerma approximation, noted a (kerma) and e (kerma), and a second without, noted a and e.

Table 6
Reference organ absorbed doses and effective dose for the neutron problem. Standard statistical uncertainties are also indicated.

	Organ absorbed doses (Gy) and effective dose (Sv)			
	Male		Female	
	Dose (Gy)	*std. unc. (%)*	*Dose (Gy)*	*std. unc. (%)*
RBM	8.74×10^{-7}	0.07	9.68×10^{-7}	0.07
Stomach	1.58×10^{-6}	0.17	1.54×10^{-6}	0.19
Testes/Ovaries	1.11×10^{-6}	0.46	9.40×10^{-7}	0.68
Liver	1.34×10^{-6}	0.12	1.46×10^{-6}	0.13
Brain	4.01×10^{-7}	0.24	5.00×10^{-7}	0.23
Skin	5.61×10^{-7}	0.04	5.79×10^{-7}	0.04
Small intestine	1.43×10^{-6}	0.11	1.50×10^{-6}	0.12
Effective dose	3.67×10^{-6} ±0.1%			

reference values.

The effective dose results, E(P), that were submitted by the participants are shown in Fig. 11 as ratios, $E(P)/E(O)$, to the reference effective dose, $E(O)$. The 1 standard deviation statistical uncertainties on the results are again not shown on the figure for clarity, but were no more than a few percent. Participant d did not calculate effective dose per se: rather than the correct sex-averaged quantity, they instead provided solutions for the male and female phantoms individually. These are shown separately on Fig. 11, noting that the male result of 0.032 and the female result of 0.028 would have given a ratio of 0.030 had averaging been applied.

No participant submitted a value for effective dose that agreed with the reference value within the accepted uncertainty. However, four participants (c, h, i and j) came to within ~20%. Such closeness was surprising for Participant i, because all their reported organ doses were very different from the reference solution; it may therefore be fair to suggest that the apparent near-success was coincidental in this case, with perhaps some fortuitous cancelling-out occurring of doses that were too high and too low. Participants a, f and k diverged from the reference solution by large amounts, being up to an order of magnitude different for Participant a; Participant d would also have diverged greatly had sex-averaging been applied. It is interesting to note that in all cases apart from Participant i, the reported value for effective dose was lower than the reference value. In fact, similar observations are also noted for many of the organ doses shown in Figs. 9 and 10. It is not clear whether these apparent patterns are simply a coincidence, or if not, what their causes or significance might be. If they are genuine, it is remarked that the use of very different cross-sections or thermal treatment options from that applied by the organizer (who assumed an O–H bond equivalent to that in light water), or even potentially the complete omission of this latter parameter by a participant, could lead to systematic differences in the results. However, because details on this choice were not requested with the submissions, such a suggestion can only be purely speculative at this stage.

In some cases, correlation was noted between organ dose agreement and effective dose agreement, whereas in other cases such correlation was not found. For example, the organ doses reported by both Participants h and j were generally around ~20% lower than those of the reference solutions, as were their estimates of effective dose; this indicates that the methods applied by those individuals for calculating effective dose were potentially correct, even though their underlying organ dose data may not have been. Conversely, all the organ doses reported by Participants c and k agreed with the reference values within uncertainty, but their effective dose estimates did not; this indicates problems with their derivations of the latter, or in the application of the correct radiation or tissue weighting factors. The effective dose estimated by Participant k was roughly a third of that of the organizer, which is close in value to 1/3.031; a suggestion could therefore be that the radiation weighting factor may not have been applied in that case. Alternatively, and recalling that the organizer found that the photon dose components were typically ~10 × higher than the neutron doses, another potential explanation might be that Participant k correctly used a value of $w_R = 3.031$ to the neutron doses but applied the 'usual' value of $w_R = 1.0$ to the photons, neglecting that the relevant radiation weighing factor for secondary radiations is that of the particle incident upon the body that generated them (i.e. the 10 keV neutron). Similarly, it may be observed that if one were to mistake the neutron energy E_n in Equation (1) as having units of eV, rather than MeV, then the ratio between the value of w_R that would result (i.e. 2.500) and that used by the organizer (i.e. 3.031) is very close to the value of $E(P)/E(O)$ seen for Participant c. Of course, these tentative explanations are purely speculative at this stage: the weighted doses for the many other organs used to determine effective dose (ICRP, 2007) were not provided by (or requested from) the participants, so such suggestions are hard to investigate further.

3.2.3. *Neutron exercise overview and observations*

The neutron intercomparison exercise may be summarized as follows:

- Eight participants from eight different countries submitted organ and effective dose results. The participants employed a range of Monte Carlo codes, data and approaches.
- Due to difficulties in defining the precise source location unambiguously, proximity to within ~10% of the reference solution was

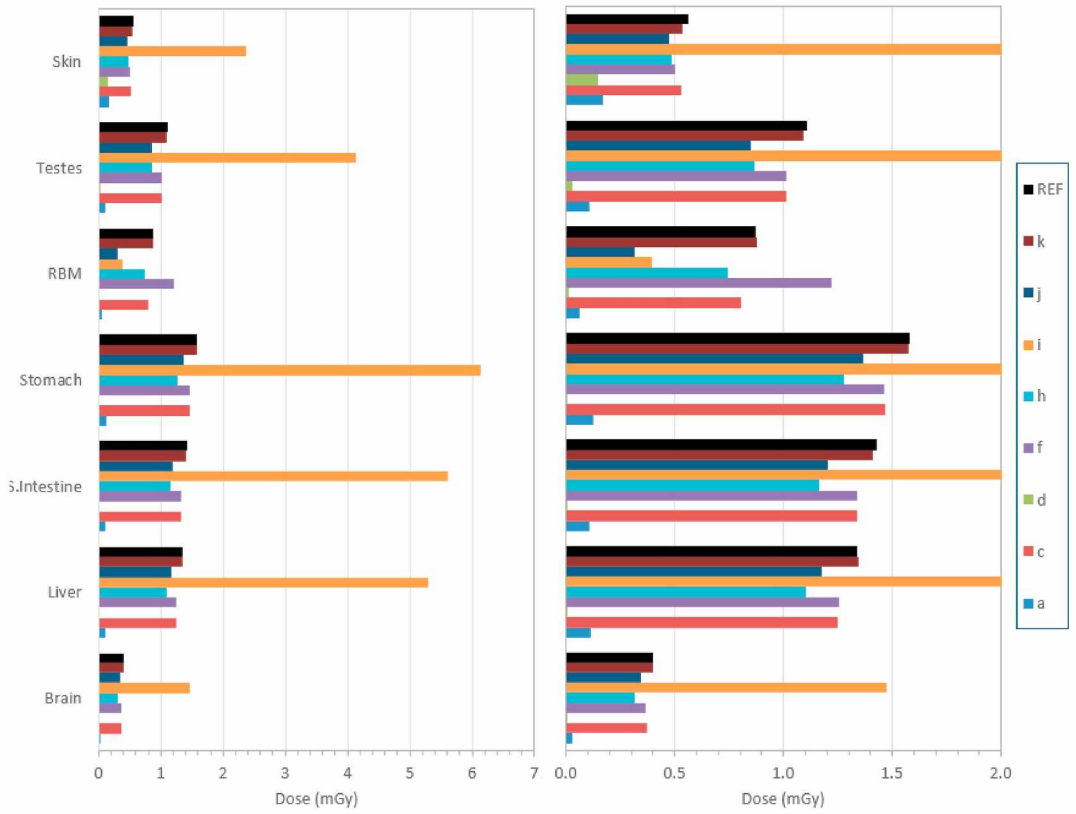

Fig. 9. Neutron point source exercise – Organ dose data submitted by the eight participants for the male phantom, compared with reference data. (Left) all data; (Right) restricted range.

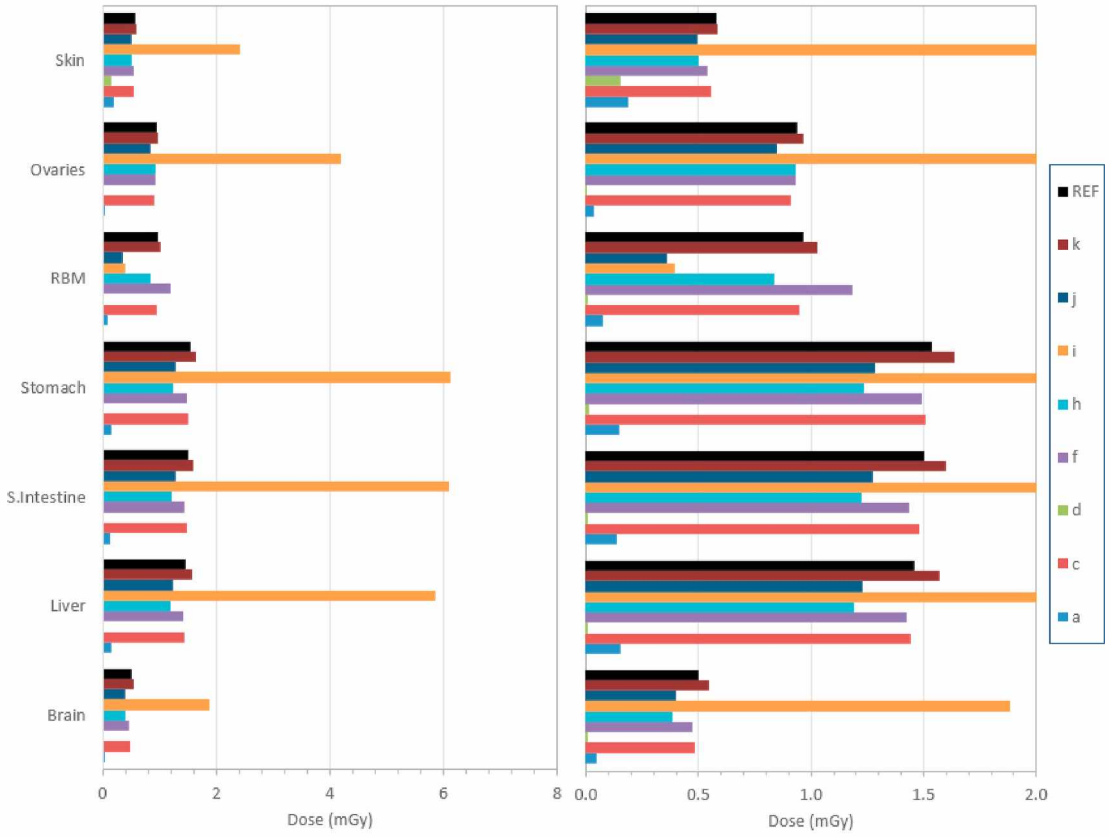

Fig. 10. Neutron point source exercise - Organ dose data submitted by the eight participants for the female phantom, compared with reference data. (Left) all data; (Right) restricted range.

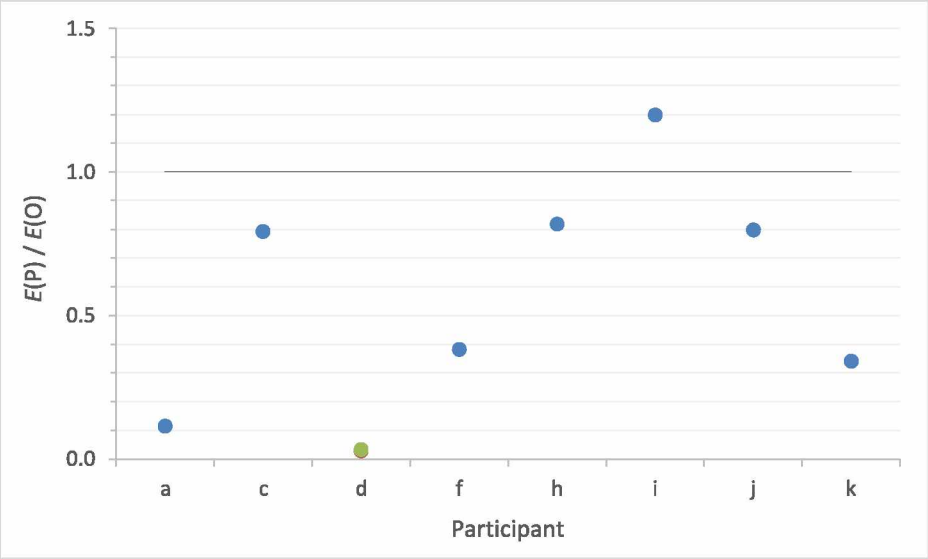

Fig. 11. Neutron point source - Ratio of effective dose data (E(P)) submitted by the participants to the reference effective dose (E(O)). Participant d erroneously provided results for the male (green) and female (red) phantoms separately. (For interpretation of the references to colour in this figure legend, the reader is referred to the Web version of this article.)

considered to indicate satisfactory agreement of a given participant's results for the purposes of analysis.

- Only two participants submitted organ doses that agreed with the reference solutions for both phantoms and all seven tissues requested for the intercomparison exercise.
- Overall, the RBM was seen to be the organ for which results were most likely to differ from the reference solution.
- No participant submitted a result for effective dose that agreed with the reference solution within uncertainty; this was inevitable in most cases, given the prior divergence of the organ dose data.

The precise causes of the divergences from the reference solutions are unknown: bespoke feedback was not provided to or by the participants, and revised solutions were not requested. However, the patterns and trends in the results indicate that, in many cases, the general types of mistake made in the photon exercises were likely being repeated in this neutron exercise. Difficulties with RBM dosimetry are an obvious example of this. However, there are still obvious differences between photon-only and neutron-photon problems. For example, the fact that the radiation weighting factor to be applied relates to the particles incident on the body, rather than the particles providing the localized energy depositions, is a non-trivial complexity that is particular to neutron simulation problems. So too is the application of the hydrogen-neutron scatter correction (i.e. 'thermal treatment') and which material is chosen as a substitute for the tissues. In addition, the radionuclide-specific neutron cross-section data are different from the elementary photon cross-section data, but the materials of the voxel phantoms are defined only on the elementary level: no data on isotopic make-ups are provided in ICRP Publication 110 (ICRP, 2009), with the optimum compositions for the tissues therefore left to individuals to decide from the options available to them. Each of these factors, and perhaps others also, will likely contribute to the observed discrepancies between the results.

3.3. *X-ray examination*

3.3.1. *Reference solution*

The coordinate system of the phantoms is as follows: The x axis is represented by the columns of the voxel array and is directed from the phantoms' right to their left side, the y axis is represented by the rows and is directed from the phantoms' front to their back, and the z axis is represented by the array slices and is directed from the feet towards the head. The origin of the coordinate system is, thus, located at the right frontal bottom border of the cuboid representing the phantom array.

The source coordinates for the reference solution for the Chest PA examination were selected as described here, and summarized also in Supplemental Table A1. The field was to be centred in height between the top and bottom extensions and laterally between the left-most and right-most extensions of the phantom's lungs. First, the minimum and maximum columns and slices containing both lungs of the reference phantoms were determined (see, e.g., Tables A2 and A.3 in ICRP Publication 110 (ICRP, 2009)). Together with the column width, the minimum and maximum columns were used to evaluate the minimum and maximum x-coordinates of the lungs, and the arithmetic mean of these two coordinates was defined as the x-coordinate of the source. The same procedure was also applied for the minimum and maximum slices, together with the slice thickness, to arrive at the central z-coordinate of the lungs and, hence, the z-coordinate of the X-ray source. Then, the slice was determined in which this z-coordinate is located, and the minimum row in that slice was looked-up in the phantom data. This information was used to evaluate the minimum y-coordinate in the central lung slice, and from this the locations of the detector (10 cm away from the frontal skin) and the source (behind the phantom at a distance of 180 cm from the detector) were derived. The source coordinates were (27.25 cm, 175.34 cm, 137.2 cm) for the male and (26.89 cm, 173.905 cm, 131.41 cm) for the female reference computational phantom, respectively. It should be noted that the information about minimum and maximum columns and rows per slice is not given in ICRP Publication 110, and this may hence be a source of uncertainty of the y-coordinate of the X-ray source.

Similarly, the X-ray source coordinates for the Abdomen AP examination were determined from the specification provided (for details see Table 1). The source coordinates were (26.50 cm, −78.71 cm, 109.2 cm) for the male and (26.54 cm, −81.57 cm, 104.54 cm) for the female reference computational phantom, respectively.

The reference solution was calculated with the radiation transport program package EGSnrc (Kawrakow et al., 2009); the photon cross-section library was an updated version (Seuntjens et al., 2002) of the XCOM database (Berger and Hubbell, 1987), and the cutoff value for photons was 2 keV; for electrons, Bremsstrahlung cross sections from the National Institute of Standards and Technology (NIST) database (Seltzer and Berger, 1985, 1986) were used, and the transport history was

generally terminated when their kinetic energy fell below 20 keV, except for electrons with an initial kinetic energy below 50 keV, whose histories were followed down to 2 keV. The "three-factor method" as described in ICRP Publication 116 (ICRP, 2010), Annex D, was used for RBM dosimetry. A mass-weighted dose to spongiosa, as described in Chapter 3 of ICRP Publication 116, was evaluated as well, since this was the method applied by several of the participants.

The reference solution conversion coefficients, together with their statistical uncertainty, are presented in Table 7 and Table 8 for the Chest PA and Abdomen AP examinations, respectively.

3.3.2. *Initial solutions*

Eight participants (or groups of participants) submitted solutions for this task; in some cases, several researchers teamed up, shared the work among them and submitted a common solution together.

The following radiation transport codes were used by the participants: FLUKA, Geant4, MCNP (3 participants), PenEasy, TRIPOLI, and VMC. One participant calculated two sets of data: one made with, and one made without the kerma approximation. These agreed with each other to within 1% for most organs, and differed notably only for the thyroid (max. 6.5%) for the chest PA examination and for the kidneys (max. 16%) for the abdomen AP examinations. In the following, only the solution made with the kerma approximation is considered.

The X-ray source coordinates assessed by the participants were largely in approximate agreement with those of the reference solution. Surprisingly, the greatest differences from the reference coordinates were not found for the y-coordinates, as expected, but for the z-coordinates. For the Chest PA examination, the largest deviations of the participants' z-coordinates from the reference coordinate were −8.9 cm and 5.6 cm, respectively, for the female phantom. For the Abdomen AP examination, the largest coordinate deviations were −2.5 cm (y-coordinate, male) and −6.5 cm (z-coordinate, female). One participant used a different coordinate system, and hence for this specific solution the source coordinates could not be verified.

For the initial solutions, a large variety of deviations from the reference solutions was found. Some participants' solutions were partly within 5–10% agreement with the reference solutions, whilst some other participants' solutions were different by much larger factors, one even by two orders of magnitude (for the conversion per kerma-area product). For most participants, the deviations from the reference solutions were different for the two normalization quantities (entrance air kerma free-in-air or kerma-area product), indicating problems with conversion between the normalization quantities. Only two (for Chest PA) and three (for Abdomen AP) participants had this conversion (approximately) correct, where for one of these, the agreement of all conversion coefficients with the reference solutions was within approximately 30%, except for the RBM. For four participants, the deviations of the RBM conversion coefficients were similar to those of the other organs; one participant did not evaluate RBM doses, and for three participants, the conversion coefficients for RBM were higher than for the other organs. These latter participants evaluated RBM dose as mass-averaged spongiosa dose, which is the reason for the discrepancy. In Fig. 12, ratios of the participants' initial solutions to the reference solutions are shown for Chest PA for conversion coefficients per air kerma free-in-air at the entrance surface for the male phantom; Fig. 13 shows ratios of the participants' initial solutions to the reference solutions for Abdomen AP conversion coefficients per kerma-area product for the female phantom. Additional figures for both X-ray examinations, both normalization quantities and both phantoms are shown in Annex B, Supplemental Figure B1 to Supplemental Figure B8. In these figures, "RBM 1" refers to the reference solution using the dose-response functions of ICRP Publication 116 (i.e., the recommended method of RBM dosimetry); for "RBM 2", an alternative "reference" solution has been evaluated using mass-weighted spongiosa doses and compared against the solutions of those participants who used this approach to estimate RBM doses.

While the ranges of deviations of the participants' solutions from the reference solutions are similar for all situations, it can be seen that a larger number of solutions were in better agreement with the reference solution for the normalization per air kerma free-in-air than for the normalization per Kerma-Area-Product. It could therefore be concluded, supported also from the feedback subsequently exchanged with the participants, that several participants were not familiar with this dose quantity, i.e. the product of air kerma free-in-air at a certain distance from the source and the field size at the same distance. Since the air kerma decreases with distance from the source according to the inverse-square law, and the field size increases quadratically with distance from the source, the product of these two measures is approximately constant everywhere along the X-ray beam.

3.3.3. *Revised solutions*

All participants were informed about the general agreement/disagreement of their submitted initial solutions with the reference solutions, and were asked for additional information about their computational approach in order to understand where the problems may be.

For many participants, the degree of agreement with, or deviation from, the reference solution were generally similar for both examinations and both phantoms. In some cases, however, the conversion coefficients for selected organs showed a different behavior from the majority of other organs. Reasons for such discrepancies were found mostly to be wrong tissue material assignment, selection of a wrong organ identification number (meaning evaluating the conversion coefficients for a different organ), and sometimes even typing errors were

Table 7
Reference organ absorbed doses per entrance air kerma free in air and per Kerma-Area-Product (KAP) and standard statistical uncertainties for the Chest PA examination.

Organ	Male			Female		
	Organ absorbed dose per		Standard statistical uncertainty	Organ absorbed dose per		Standard statistical uncertainty
	Entrance air kerma free in air	KAP		Entrance air kerma free in air	KAP	
	Gy/Gy	Gy/(Gy cm^2)	(%)	Gy/Gy	Gy/(Gy cm^2)	(%)
RBM	0.1613	1.943E-04	0.04	0.2176	2.547E-04	0.04
Mass-weighted spongiosa average	0.2529	3.046E-04	0.04	0.3212	3.761E-04	0.04
Lungs	0.4257	5.127E-04	0.03	0.654	7.658E-04	0.03
Stomach	0.1959	2.359E-04	0.14	0.2482	2.906E-04	0.13
Breast	0.07592	9.143E-05	0.53	0.1522	1.782E-04	0.09
Heart	0.28	3.371E-04	0.08	0.4088	4.786E-04	0.08
Oesophagus	0.2915	3.510E-04	0.23	0.3935	4.607E-04	0.21
Thyroid	0.2061	2.482E-04	0.39	0.2596	3.040E-04	0.38

Table 8
Reference organ absorbed doses per entrance air kerma free in air and per Kerma-Area-Product (KAP) and standard statistical uncertainties for the Abdomen AP examination.

Organ	Male			Female		
	Organ absorbed dose per		Standard statistical uncertainty	Organ absorbed dose per		Standard statistical uncertainty
	Entrance air kerma free in air	KAP		Entrance air kerma free in air	KAP	
	Gy/Gy	Gy/(Gy cm^2)	(%)	Gy/Gy	Gy/(Gy cm^2)	(%)
RBM	0.09041	1.048E-04	0.04	0.1153	1.342E-04	0.04
Mass-weighted spongiosa average	0.1511	1.751E-04	0.04	0.1893	2.203E-04	0.04
Liver	0.2373	2.749E-04	0.03	0.382	4.446E-04	0.03
Kidneys	0.1348	1.562E-04	0.11	0.2463	2.867E-04	0.09
Pancreas	0.349	4.044E-04	0.1	0.4995	5.813E-04	0.09
Small intestine	0.5699	6.603E-04	0.04	0.5726	6.664E-04	0.04
Colon	0.5309	6.152E-04	0.05	0.6533	7.603E-04	0.04
Bladder wall	0.5134	5.949E-04	0.14	0.7083	8.243E-04	0.13

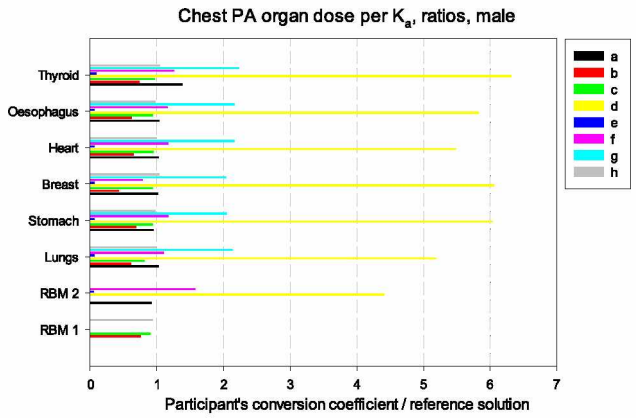

Fig. 12. X-ray examination exercise - Ratios of participants' initial dose conversion coefficients per air kerma free in-air to the respective reference solutions for the Chest PA examination of the male phantom.

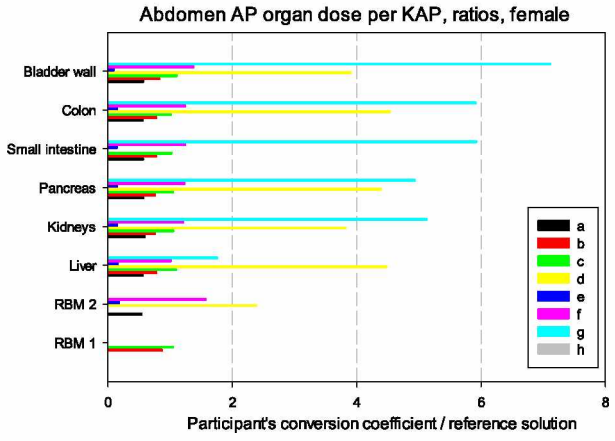

Fig. 13. X-ray examination exercise - Ratios of participants' initial dose conversion coefficients per Kerma-Area-Product to the respective reference solutions for the Abdomen AP examination of the female phantom.

made when introducing the results into the provided templates.

Some errors concerning evaluation of air kerma were the following: some participants evaluated the entrance air kerma including backscatter; one participant evaluated air kerma free-in-air at a fixed distance from the source (1 m) instead of at the source-to-skin distance; and one had a wrong material definition for the detector used to score air kerma.

All participants except Participant f made use of the opportunity to revise their submitted solutions following feedback from the organizer. The revisions included correction of the above-mentioned problems, and one participant also made adjustments in the source position. The larger differences in the source coordinates reported above for the initial submission, however, were not corrected. There were some cases where the "corrections" applied helped to get rid of one set of the discrepancies in the original submission but worsened other parts. Unfortunately, not all participants provided explanations of exactly what they changed in their computational procedure to arrive at their revised solutions.

The revised solutions are illustrated in Fig. 14, Fig. 15 and Supplemental Figure B9 to Supplemental Figure B14. It can be seen that the largest outliers have been successfully removed, but there are still many solutions that differ by more than 20% from the reference solution – in either direction.

4. Summary, discussion and conclusions

In the framework of EURADOS working group 6 on computational dosimetry, an intercomparison was organized on the use of the ICRP Reference Computational Phantoms with radiation transport codes. Solutions for three out of the six exercises proposed in (Zankl et al., 2021a) have been analyzed in this paper. The participants employed a

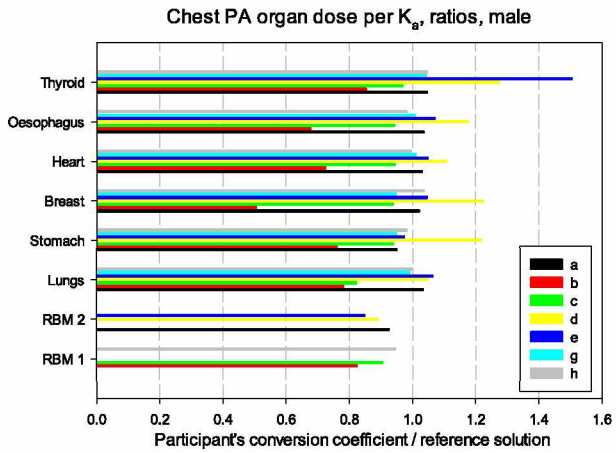

Fig. 14. X-ray examination exercise - Ratios of participants' revised dose conversion coefficients per air kerma free-in-air to the respective reference solutions for the Chest PA examination of the male phantom.

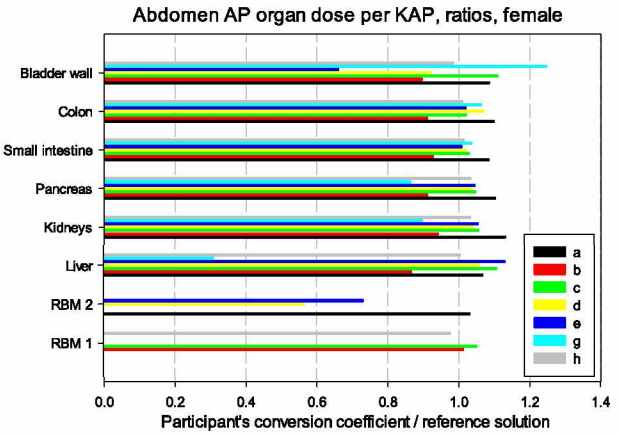

Fig. 15. X-ray examination exercise - Ratios of participants' revised dose conversion coefficients per Kerma-Area-Product to the respective reference solutions for the Abdomen AP examination of the female phantom.

range of Monte Carlo codes (FLUKA, Geant4, MCNP family codes, PenEasy, TRIPOLI and VMC), data and approaches.

For the three exercises, difficulties in defining the precise source location were encountered because the instructions that were provided gave rise to inevitable ambiguities. Consequently, proximity to within ~10% of the reference solution was considered to be satisfactory agreement for a given participant's results. Although some participants provided initial solutions that were in good agreement with the reference solutions, for many of the others differences of several tens of percent, or even several orders of magnitude, were exhibited. Of all the organs, the RBM caused the most discrepancy, both in terms of general magnitude and frequency. Given the more complex dosimetry of the RBM compared to the other organs (ICRP, 2010), participants often had problems in correctly implementing the ICRP-recommended bone dosimetry method in their practical applications. Following this general finding, it was decided to have a specific article that describes the ICRP bone dosimetry method in more detail and provides practical guidance and technical hints for incorporating this method into various types of radiation transport codes (Zankl et al., 2021b).

Following feedback and suggestions from the organizers for the photon exercises, revised solutions were submitted by some of the participants; in general, agreement was improved. However, not all participants provided a revised solution, and not all discrepancies were able to be explained. Some errors were evidently due to a lack of care, such as copy-and-paste errors. Sometimes there was a misunderstanding concerning the normalization quantity or a wrong definition of the source. However, in some cases the participants did not give any details about the changes that they had made to obtain their revised solution. On the whole, most participants succeeded in finding their errors by themselves, but for some of the others additional help from the organizers was needed. It is also clear that some of the errors could have been avoided with more thorough quality assurance (QA) checks by participants. For instance, the participants could have compared their results with available literature data for similar exposure conditions. Similarly, those participants whose datasets contained a result for one of the organs that differed from those for all the other organs by a very large degree ought perhaps to have identified that outcome as being physically implausible, and hence could also have noticed their error had greater QA checks been performed.

Feedback was not provided for the neutron problem, because every participant who contributed a solution had also contributed to at least one of the other exercises and in many cases the same errors were likely being repeated. However, one difference from the photon exercises might have originated from incorrect use of the radiation weighting factor (w_R) for neutron exposures. Differences in the assumed isotopic compositions of the various tissue materials within the phantom, and also differences in the choices for their thermal treatment cross-sections, may also have led to discrepancies between the participants' and organizer's results. Although two participants submitted organ doses that agreed with the reference solutions for both phantoms and all seven tissues requested for the neutron intercomparison exercise, no participant submitted a result for effective dose that agreed with the reference solution within uncertainty. This could suggest an error in the derivation of effective dose from organ doses, with misinterpretation of how to determine the radiation weighting factor (Equation (1)), or its use for both the neutron and photon dose components, being speculated as conceivable causes.

Overall, it is clear that some of the errors made by the various participants were common across the three exercises. These include difficulties with RBM dosimetry, difficulties in correctly defining the source, and presumed typographical mistakes in copying-and-pasting of results. Conversely, however, some errors were specific to the individual exercises themselves, and hence to the unique exposure scenarios of interest. These include mistakes in organ dosimetry (e.g. miscalculation of absorbed dose for organs having multiple tissues), difficulties with normalization (e.g. to Kerma-Area-Product), or problems with correctly deriving effective doses in scenarios featuring multiple particle species (e.g. misapplying radiation weighting factors to photon/neutron components). Whilst the former set of errors may serve as general lessons-learnt, the latter type demonstrates the complexities of voxel phantom calculations and the scenarios in which they are typically employed. In turn, it may be inferred that the successful application of these phantoms by an individual in one particular circumstance cannot be taken to guarantee successful application by that same individual in a different circumstance. The value of thorough QA of all input files and all results is therefore again emphasized.

The above observations are important, and also perhaps surprising: although the scope of the WG6 intercomparison project was nominally intended to be just a study into the implementation of voxel phantoms, many of the mistakes made by participants were not related to that per se. In fact, the various exercises have highlighted wider issues regarding the usage of Monte Carlo codes, correct modelling of exposure scenarios, dosimetry, and general approaches to QA in computational radiological protection. To that end, the results and conclusions shown in the current paper demonstrate the needs, as well as the benefits, of these kinds of exercise. In addition to providing additional benchmarked data to the participants, they demonstrate the difficulties encountered by individuals in correctly implementing Monte Carlo modelling and some of the methods recommended by ICRP, as well as supplying an invaluable resource of reference scenarios and results that future novice users may employ for training purposes. Finally, lessons can also be learned for future intercomparison exercises. As a matter of fact, even if the organizers were extremely cautious in defining and describing the problems, some participants errors could perhaps have been avoided with additional guidance. For instance, it could be useful in future exercises to define the dosimetric quantities used and to provide a list of checks to be done by the participants.

Declaration of competing interest

The authors declare that they have no known competing financial interests or personal relationships that could have appeared to influence the work reported in this paper.

Appendix A. Supplementary data

Supplementary data to this article can be found online at https://doi.org/10.1016/j.radmeas.2021.106695.

References

Agostinelli, S., Allison, J., Amako, K., Apostolakis, J., Araujo, H., Arce, P., Asai, M., Axen, D., Banerjee, S., Barrand, G., Behner, F., Bellagamba, L., Boudreau, J., Broglia, L., Brunengo, A., Burkhardt, H., Chauvie, S., Chuma, J., Chytracek, R., Cooperman, G., Cosmo, G., Degtyarenko, P., Dell'Acqua, A., Depaola, G., Dietrich, D., Enami, R., Feliciello, A., Ferguson, C., Fesefeldt, H., Folger, G., Foppiano, F., Forti, A., Garelli, S., Giani, S., Giannitrapani, R., Gibin, D., Gómez Cadenas, J.J., González, I., Gracia Abril, G., Greeniaus, G., Greiner, W., Grichine, V., Grossheim, A., Guatelli, S., Gumplinger, P., Hamatsu, R., Hashimoto, K., Hasui, H., Heikkinen, A., Howard, A., Ivanchenko, V., Johnson, A., Jones, F.W., Kallenbach, J., Kanaya, N., Kawabata, M., Kawabata, Y., Kawaguti, M., Kelner, S., Kent, P., Kimura, A., Kodama, T., Kokoulin, R., Kossov, M., Kurashige, H., Lamanna, E., Lampén, T., Lara, V., Lefebure, V., Lei, F., Liendl, M., Lockman, W., Longo, F., Magni, S., Maire, M., Medernach, E., Minamimoto, K., Mora de Freitas, P., Morita, Y., Murakami, K., Nagamatu, M., Nartallo, R., Nieminen, P., Nishimura, T., Ohtsubo, K., Okamura, M., O'Neale, S., Oohata, Y., Paech, K., Perl, J., Pfeiffer, A., Pia, M.G., Ranjard, F., Rybin, A., Sadilov, S., Di Salvo, E., Santin, G., Sasaki, T., Savvas, N., Sawada, Y., Scherer, S., Sei, S., Sirotenko, V., Smith, D., Starkov, N., Stoecker, H., Sulkimo, J., Takahata, M., Tanaka, S., Tcherniaev, E., Safai Tehrani, E., Tropeano, M., Truscott, P., Uno, H., Urban, L., Urban, P., Verderi, M., Walkden, A., Wander, W., Weber, H., Wellisch, J.P., Wenaus, T., Williams, D.C., Wright, D., Yamada, T., Yoshida, H., Zschiesche, D., 2003. Geant4—a simulation toolkit. Nucl. Instrum. Methods Phys. Res. Sect. A Accel. Spectrom. Detect. Assoc. Equip. 506 (3), 250–303.

Battistoni, G., Muraro, S., Sala, P.R., Cerutti, F., Ferrari, A., Roesler, S., Fasso, A., Ranft, J., 2006. The FLUKA code: description and benchmarking. In: Albrow, M., Raja, R. (Eds.), Hadronic Shower Simulation Workshop. AIP Conference Proceeding, Fermi National Accelerator Laboratory (Fermilab), Batavia, Illinois, pp. 31–49.

Berger, M.J., Hubbell, J.H., 1987. XCOM: Photon Cross Sections on a Personal Computer. National Bureau of Standards (former name of NIST), Gaithersburg, MD.

Brun, E., Damian, F., Diop, C.M., Dumonteil, E., Hugot, F.X., Jouanne, C., Lee, Y.K., Malvagi, F., Mazzolo, A., Petit, O., Trama, J.C., Visonneau, T., Zoia, A., 2015. Tripoli-4®, CEA, EDF and AREVA reference Monte Carlo code. Ann. Nucl. Energy 82, 151–160.

Hunt, J.G., da Silva, F.C., Mauricio, C.L., dos Santos, D.S., 2004. The validation of organ dose calculations using voxel phantoms and Monte Carlo methods applied to point and water immersion sources. Radiat. Protect. Dosim. 108 (1), 85–89.

ICRP, 2007. The 2007 recommendations of the international commission on radiological protection. ICRP publication 103. Ann. ICRP 37 (2–4).

ICRP, 2009. Adult reference computational phantoms. ICRP Publication 110. Ann. ICRP 39 (2).

ICRP, 2010. Conversion coefficients for radiological protection quantities for external radiation exposures. ICRP publication 116. Ann. ICRP 40 (2–5).

Kawrakow, I., Mainegra-Hing, E., Rogers, D.W.O., Tessier, F., Walters, B.R.B., 2009. The EGSnrc Code System: Monte Carlo Simulation of Electron and Photon Transport. National Research Council of Canada (NRCC), Ottawa.

Rabus, H., Gómez Ros, J.-M., Villagrasa, C., Eakins, J.S., Vrba, T., Blideanu, V., Zankl, M., Tanner, R., Struelens, L., Brkic, H., Domingo, C., Baiocco, G., Caccia, B., Huet, C., Ferrari, P., 2021. Quality assurance for the use of computational methods in dosimetry: activities of EURADOS Working Group 6 'Computational Dosimetry. J. Radiol. Prot. 41, 46–58.

Seltzer, S.M., Berger, M.J., 1985. Bremsstrahlung spectra from electron interactions with screened atomic nuclei and orbital electrons. Nucl. Instrum. Methods Phys. Res., Sect. B 12, 95–134.

Seltzer, S.M., Berger, M.J., 1986. Bremsstrahlung energy spectra from electrons with kinetic energy from 1 keV to 10 GeV incident on screened nuclei and orbital electrons of neutral atoms with Z=1-100. Atomic Data Nucl. Data Tables 35, 345–418.

Sempau, J., Badal, A., Brualla, L., 2011. A PENELOPE-based system for the automated Monte Carlo simulation of clinacs and voxelized geometries-application to far-from-axis fields. Med. Phys. 38 (11), 5887–5895.

Seuntjens, J.P., Kawrakow, I., Borg, J., Hobeila, F., Rogers, D.W.O., 2002. Calculated and measured air-kerma response of ionization chambers in low and medium energy photon beams. In: Seuntjens, J.P., Mobit, P. (Eds.), Recent Developments in Accurate Radiation Dosimetry, Proc. Of an Int'l Workshop. Medical Physics Publishing, Madison, USA, pp. 69–84.

Werner, C.J., Armstrong, J., Brown, F.B., Bull, J.S., Casswell, L., Cox, L.J., Dixon, D., Forster, R.A., Goorley, J.T., Hughes, H.G., Favorite, J., Martz, R., Mashnik, S.G., Rising, M.E., Solomon, C., Sood, A., Sweezy, J.E., Zukaitis, A., Anderson, C., Elson, J. S., Durkee, J.W., Johns, R.C., McKinney, G.W., McMath, G.E., Hendricks, J.S., Pelowitz, D.B., Prael, R.E., Booth, T.E., James, M.R., Fensin, M.L., Wilcox, T.A., Kiedrowski, B.C., 2017. MCNP User's Manual, Code Version 6.2. Los Alamos National Security, LLC. LA-UR-17-29981. October 27.

Zankl, M., Eakins, J.S., Gómez Ros, J.-M., Huet, C., Jansen, J., Moraleda, M., Reichelt, U., Struelens, L., Vrba, T., 2021a. EURADOS intercomparison on the usage of the ICRP/ICRU adult reference computational phantoms. Radiat. Meas. 145, 106596.

Zankl, M., Eakins, J.S., Gómez Ros, J.-M., Huet, C., 2021b. The ICRP recommended methods of red bone marrow dosimetry. Radiat. Meas. 146, 106611.